Simulated microgravity-induced mitochondrial dysfunction in rat cerebral arteries

Ran Zhang,*[,1] Hai-Hong Ran,[†,1] Li-Li Cai,[‡,1] Li Zhu,[‖] Jun-Fang Sun,* Liang Peng,* Xiao-Juan Liu,* Lan-Ning Zhang,* Zhou Fang,* Yong-Yan Fan,* and Geng Cui[§,1,2]

*Institute of Geriatric Cardiology, [†]Department of Geriatric Hematology, [‡]Department of Clinical Laboratory Medicine, and [§]Department of Osteology, Chinese People's Liberation Army General Hospital, Beijing, China; and [‖]Changhai Hospital, Second Military Medical University, Shanghai, China

ABSTRACT **Exposure to microgravity results in cardiovascular deconditioning, and cerebrovascular oxidative stress injury has been suggested to occur. To elucidate the mechanism for this condition, we investigated whether simulated microgravity induces mitochondrial dysfunction in rat arteries. Four-week hindlimb unweighting (HU) was used to simulate microgravity in rats. Mitochondrial reactive oxygen species (ROS), mitochondrial membrane potential ($\Delta\psi m$), mitochondrial permeability transition pore (mPTP) opening, mitochondrial respiratory control ratio (RCR), MnSOD/GPx activity and expression, and mitochondrial malondialdehyde (MDA) were examined in rat cerebral and mesenteric VSMCs. Compared with the control rats, mitochondrial ROS levels, mPTP opening, and MDA content increased significantly ($P<0.001$, $P<0.01$, and $P<0.01$, respectively), $\Delta\psi m$, RCR, MnSOD/GPx activity ($P<0.001$ for $\Delta\psi m$ and RCR; $P<0.05$ for MnSOD; and $P<0.001$ for GPx activity) and protein abundance of mitochondrial MnSOD/GPx-1 decreased ($P<0.001$ for MnSOD and GPx-1) in HU rat cerebral but not mesenteric arteries. Chronic treatment with NADPH oxidase inhibitor apocynin and mitochondria-targeted antioxidant mitoTempol promoted recovery of mitochondrial function in HU rat cerebral arteries, but exerted no effects on HU rat mesenteric arteries. Therefore, simulated microgravity resulted in cerebrovascular mitochondrial dysfunction, and crosstalk between NADPH oxidase and mitochondria participated in the process.—Zhang, R., Ran, H.-H., Cai, L.-L, Zhu, L., Sun, J.-F., Peng, L., Liu, X.-J., Zhang, L.-N., Fang, Z., Fan, Y.-Y., Cui, G. Simulated microgravity induced mitochondrial dysfunction in rat cerebral arteries. *FASEB J.* 28, 2715–2724 (2014). www.fasebj.org**

Key Words: hindlimb unweighting · oxidative stress · NADPH oxidase

Exposure to microgravity results in postflight cardiovascular deconditioning in astronauts. Both spaceflight and ground-based human studies and simulated microgravity animal studies have reported adaptive changes in vascular structures and functions in cardiovascular deconditioning. However, despite research on the subject (1–4), the mechanism for this process remains to be identified.

When simulated microgravity induced by hindlimb unweighting (HU) was performed, differential structural and functional changes were reported to occur in cerebral and mesenteric arteries (1, 2, 5, 6). Proliferation, apoptosis, and ion-channel remodeling of vascular smooth muscle cells (VSMCs), endothelial inflammation, and nitric oxide synthase (NOS)–nitric oxide (NO) system regulation have been indicated in this process (7–13). The pathophysiological roles of the local renin–angiotensin system (L-RAS) are observed not only in cardiovascular disorders but also in cardiovascular alterations during simulated microgravity (14, 15). The expression of angiotensin II (Ang II) and Ang II type 1 receptor (AT_1R), the key components of RAS, increased and decreased in HU rat cerebral and femoral arteries, respectively (14). L-RAS plays pivotal roles in differential structural changes in large- and medium-sized arteries from the fore and hind body parts of HU rats (15), and blockade of AT_1R with losartan partially restored cerebrovascular responses to vasoconstrictors and vasodilators, which were related to the regulation of the NOS-NO system (16). We also observed increased superoxide anion ($O_2^{\cdot -}$) levels in HU rat cerebral arteries, which were attenuated by losartan (16, 17). In another work (data did not shown), we

Abbreviations: $\Delta\psi m$, mitochondrial membrane potential; Ang II, angiotensin II; Apo, apocynin; AT_1R, angiotensin II type 1 receptor; BSA, bovine serum albumin; Con, control; GPx, glutathione peroxidase; GPx-1, glutathione peroxidase-1; HU, hindlimb unweighting; MDA, malondialdehyde; L-RAS, local renin–angiotensin system; MFI, mean fluorescence intensity; MnSOD, manganese superoxide dismutase; mPTP, mitochondrial permeability transition pore; MT, mitoTempol; NO, nitric oxide; NOS, nitric oxide synthase; RAS, renin–angiotensin system; RCR, respiratory control ratio; ROS, reactive oxygen species; SOD, superoxide dismutase; TMRM, tetramethyl rhodamine methyl ester; VSMC, vascular smooth muscle cell

[1] These authors contributed equally to this work.

[2] Correspondence: Department of Osteology, Chinese People's Liberation Army General Hospital, 28 Fuxing Rd., Beijing 100853, China. E-mail: bjzhangran@126.com

doi: 10.1096/fj.13-245654

found that NADPH oxidase activity was enhanced by HU in rat cerebral arteries, by the NADPH oxidase inhibitor apocynin (Apo). Although this phenomenon may be associated with NADPH oxidase activation, it is still uncertain whether other cellular mechanisms are involved in vascular oxidative injury induced by microgravity.

Mitochondria are the most important sources of reactive oxygen species (ROS) and interact with NADPH oxidase in vascular oxidative stress injury (18, 19). Mitochondrial dysfunction has been well studied in oxidative stress injury and cardiovascular disorders (20). Mitochondria have an abundance of antioxidants, such as superoxide dismutase (SOD), catalase, and glutathione peroxidase (GPx), which are involved in maintaining mitochondrial structural and functional integrity (20–22). Mitochondrial dysfunction and oxidative injury are characterized by decreased expression and activity of SOD and GPx in the heart and kidney (21–23). Simulated microgravity for 72 h produced morphologic changes, with mitochondrial disassembly and organelle/cytoplasmic NADPH redistribution in cultured vascular endothelial cells (24). Endothelial dysfunction, cardiovascular remodeling, and inflammation through mitochondrial dysfunction have been well documented (25). However, whether mitochondrial dysfunction participates in vascular oxidative stress injury during microgravity and whether differential mitochondrial dysfunction exists in HU rat cerebral and mesenteric arteries both remain to be determined.

In the current study, we investigated whether simulated microgravity induces mitochondrial dysfunction in rat cerebral and mesenteric arterial VSMCs. To investigate the mechanism, chronic treatments with the NADPH oxidase inhibitor Apo and the mitochondria-targeted antioxidant mitoTempol (MT) were used to determine whether there is crosstalk between NADPH oxidase and mitochondria in vascular mitochondrial dysfunction during simulated microgravity.

MATERIALS AND METHODS

Rats and tissue treatment

The handling and treatment of the rats were in accordance with the Guiding Principles for the Care and Use of Animals in the Field of Physiological Sciences and met Chinese guidelines for experimental animals.

Male Sprague-Dawley rats were randomly assigned to 6 groups (n=8/group): control (Con), HU, HU + Apo, HU + MT, Con + Apo, and Con + MT. HU + Apo, HU +MT, Con + Apo, and Con + MT rats received distilled water containing Apo at 50 mg/kg/d or MT at 0.7 mg/kg/d by gavage, respectively. Rats in the other groups received an equal volume of vehicle (distilled water). The technique for HU has been published in detail (10) and was used to simulate microgravity in rats.

After 28 d of treatment, each rat was anesthetized with pentobarbital sodium (40 mg/kg, intraperitoneally) and killed by exsanguination *via* the abdominal aorta. Cerebral and mesenteric arteries were rapidly removed and placed in cold Krebs buffer solution containing 118.3 mM NaCl, 14.7 mM KCl, 1.2 mM KH_2PO_4, 1.2 mM $MgSO_4 \cdot 7H_2O$, 2.5 mM $CaCl_2 \cdot 2H_2O$, 25 mM $NaHCO_3$, 11.1 mM dextrose, and 0.026 mM EDTA (pH 7.4).

Mitochondria isolation

Mitochondria of rat cerebral and mesenteric arterial VSMCs were isolated by using a kit according to the manufacturer's instructions (Pierce, Rockford, IL, USA). For single cell isolation, VSMCs were dissociated from cerebral and mesenteric arteries as described elsewhere (8, 9). Briefly, samples were pelleted by centrifugation of the harvested cell suspensions at 850 *g* for 2 min before mitochondria isolation reagents A, B, and C were added in the correct sequence. The mixture was centrifuged at 700 *g* for 10 min at 4°C, and the supernatant at 12,000 *g* for 15 min at 4°C. Mitochondria isolation reagent C was added to the pellet and centrifuged at 12,000 *g* for 5 min before the pellet was resuspended in 80 mM sucrose with 0.1% bovine serum albumin (BSA). Mitochondrial fractions were kept at 4°C and studied within 3 h of isolation. A protein content assay (Bio-Rad, Hercules, CA, USA) was performed on the isolated mitochondria fractions. The purity of the mitochondrial fractions was confirmed by Western blot using antibodies against protein markers specific for plasma membrane (GAPDH) and mitochondria (cytochrome *c*, COX-IV, and HSP70).

Mitochondrial ROS assay

Mitochondria isolated from rat cerebral and mesenteric arterial VSMCs were diluted to 2 mg protein/ml in assay medium and incubated with 10 μM DCFH-DA (Molecular Probes, Inc., Eugene, OR, USA) for 10 min at 25°C, during which process DCFH-DA was hydrolyzed by endogenous esterases to DCFH. The suspension was then diluted 10-fold and centrifuged at 9000 *g* for 5 min to remove the external probe. The final pellet was resuspended in 80 mM sucrose with 0.1% BSA. DCFH-DA-loaded mitochondria were analyzed by a fluorospectrophotometer (F4000; Hitachi Corp, Tokyo Japan) at 488 nm excitation and 525 nm emission. Data are expressed as the fluorescence intensity per milligram protein.

Mitochondrial membrane potential ($\Delta\psi m$) assay

$\Delta\psi m$ was detected with a fluorescent probe, tetramethyl rhodamine methyl ester (TMRM; Molecular Probes Inc.), which reversibly accumulates according to the membrane potential. Briefly, isolated cerebral and mesenteric artery VSMCs were incubated in HEPES buffer (134 mM NaCl, 6 mM KCl, 2 mM $CaCl_2$, 1 mM $MgCl_2$, 10 mM HEPES, and 10 mM glucose, pH 7.4) containing TMRM (100 nM) for 30 min, followed by a 15-min wash. Flow cytometric analysis (FACSCalibur Flow Cytometer; BD Biosciences, San Diego CA, USA) was performed to analyze mean fluorescence intensity (MFI).

Mitochondrial permeability transition pore (mPTP) opening assay

A commercially available kit (Genmed Scientifics Inc., Wilmington, DE, USA) was used to investigate the mPTP opening, according to the manufacturer's instructions. Briefly, mitochondria isolated from cerebral and mesenteric arterial VSMCs were seeded in 96-well plates. Mitochondrial fractions were incubated with reagent A at 37°C for 1 min. mPTP opening was determined by an absorbance decrease in light

scattering at 540 nm, by using a UV-visible spectrophotometer (UV-2550; Shimadzu, Kyoto, Japan). Results were calculated as the value of sample minus background.

Mitochondrial respiratory control ratio (RCR)

Another kit from Genmed Scientifics Inc. was used to investigate the mitochondrial RCR, according to the instructions provided. RCR was measured at 25°C. Briefly, mitochondrial fractions were incubated with Genmed reagent A. State 4 substrate solution (reagent B) and state 3 substrate solution (reagent C) were added in the proper sequence. Mitochondrial state 3 and state 4 respiration rates were determined, and mitochondrial RCR was calculated as RCR = state 3 respiration rate/state 4 respiration rate.

Manganese SOD (MnSOD) and GPx activity in mitochondria

MnSOD activity was determined with a commercially available kit (Calbiochem, La Jolla, CA, USA), according to the manufacturer's instructions. Briefly, mitochondrial fractions were incubated with 1-methyl-2-vinylpyridinium in assay buffer at 37°C for 1 min. After the substrate 5,6,6α,11β-tetrahydro-3,9,10-trihydroxybenzo(c)fluorine was added, the absorbance at 525 nm was recorded. MnSOD activity was determined from the ratio of the autooxidation rates measured in the presence (sample) and in the absence (blank) of MnSOD. The results are expressed as units per milligram of mitochondrial protein.

GPx activity was measured with a commercially available kit (Calbiochem), according to the manufacturer's instructions. Briefly, mitochondrial fractions were incubated with a solution containing 1 mM GSH, ≥0.4 U/ml glutathione reductase, and 0.2 mM NAD(P)H. The reaction was initiated by adding the substrate *tert*-butyl hydroperoxide, and the absorbance at 340 nm was recorded. The results are expressed as units per milligram of mitochondrial protein.

Western blot analysis of mitochondrial MnSOD, GPx-1, and protein markers

Western blot was used to identify protein abundance in mitochondrial fractions of VSMCs. Briefly, proteins in mitochondrial fractions were separated on SDS-polyacrylamide gels and transferred to nitrocellulose membranes. The membranes were incubated with proper primary antibodies (Abcam, Cambridge, MA, USA) for the proteins of interest: anti-cytochrome *c* (1:1000), anti-COX IV (1:1000), anti-Hsp70 (1:1000), anti-GAPDH (1:500), anti-MnSOD (1:1000), anti-GPx-1 (1:1000), and anti-Porin (1:1000) at 4°C overnight. Then, the membranes were washed and incubated with the appropriate horseradish peroxidase (HRP)–conjugated secondary antibodies for 2 h at room temperature. The enhanced chemiluminescence detection reagents (Amersham, Cleveland, OH, USA) were added after the membranes were washed, and the membranes were exposed to Hyperfilm (Amersham).

Mitochondrial lipid peroxidation assay

Malondialdehyde (MDA) is a sensitive marker of lipid peroxidation. A mitochondrial MDA assay was performed with a commercially available kit (Calbiochem), according to the manufacturer's instructions. Briefly, mitochondrial fractions were resuspended in 5 mM butylated hydroxytoluene. For each reaction, 200 μl of mitochondria sample or standard was added to 650 μl chromogenic reagents and 150 μl of 12 N HCl at 45°C for 60 min. The samples were then centrifuged at 10,000 *g* for 5 min at 4°C and the supernatant collected. The absorbance at 525 nm was recorded. The level of mitochondrial MDA was calculated by using a standard curve.

Statistical analysis

Results are expressed as means ± SEM. Prism 5.0 (GraphPad, San Diego, CA, USA) was used for statistical analyses and figure presentation. Statistical evaluation was performed using 1-way ANOVA. Values of $P < 0.05$ were considered statistically significant.

RESULTS

General data

Microgravity simulated by HU resulted in a significantly lower soleus muscle mass ($P<0.001$). Soleus muscle-to-body mass ratios were significantly reduced ($P<0.001$) in the HU, HU + Apo, and HU + MT rats, which confirmed the efficacy of simulated microgravity and the reliability of the animal model used. Data are summarized in **Table 1**. As for the methodology, the positive expression of cytochrome *c*, COX-IV, and HSP70 and the negative expression of GADPH in the mitochondrial fractions (**Fig. 1**) guaranteed the reliability of the mitochondrial fractions used in the current study.

Effects of HU on mitochondrial ROS

To investigate whether HU causes mitochondrial oxidative injury, mitochondrial ROS levels were detected in rat cerebral and mesenteric arterial VSMCs (**Fig. 2**). Four weeks of HU increased ROS generation in rat

TABLE 1. *Body mass, soleus mass, and soleus:body mass ratio of rats by study group*

Group	Initial mass (g)	Final mass (g)	Soleus mass (mg)	Soleus:body mass (mg/g)
Con	199.33 ± 4.62	345.20 ± 18.12	134.62 ± 4.87	0.39 ± 0.02
HU	198.85 ± 4.41	344.15 ± 17.76	65.41 ± 2.69***	0.19 ± 0.01***
Con + Apo	201.53 ± 4.66	342.65 ± 17.71	138.36 ± 2.85	0.40 ± 0.01
HU + Apo	199.87 ± 4.52	340.79 ± 18.56	74.11 ± 3.39***	0.21 ± 0.02***
Con + MT	199.64 ± 4.33	340.93 ± 16.14	139.83 ± 4.23	0.41 ± 0.01
HU + MT	199.31 ± 4.58	342.82 ± 18.63	75.52 ± 3.54***	0.22 ± 0.02***

Values are means ± SEM (n=8/group). ***$P < 0.001$ *vs.* control.

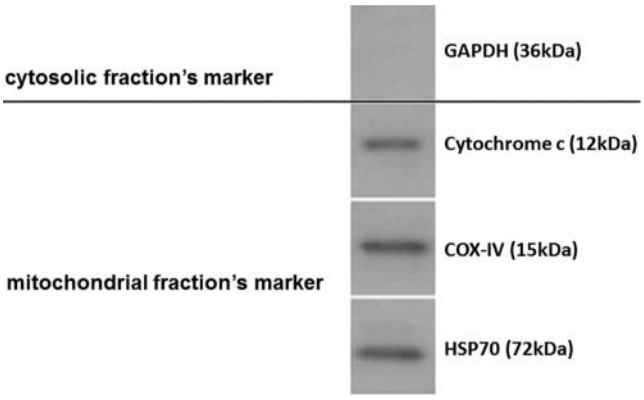

Figure 1. Western blot analysis of mitochondrial fractions probed with antibodies directed toward GAPDH, cytochrome *c*, COX-IV, and HSP70.

cerebral arteries ($P<0.001$) but not in mesenteric arteries, and enhanced ROS generation in the cerebral arteries by HU was suppressed by chronic treatment with Apo and MT ($P<0.01$ and $P<0.001$, respectively; Fig. 2*A*). Neither HU nor Apo or MT affected the levels of ROS in Con and Apo- or MT-treated HU rat mesenteric arteries (Fig. 2*B*).

Effects of HU on Δψm

Δψm is essential for normal mitochondrial function. We examined the effects of HU on Δψm of rat cerebral and mesenteric arterial VSMCs (**Fig. 3**). HU diminished cerebrovascular Δψm ($P<0.001$), which was blunted by chronic treatment with Apo or MT ($P<0.01$ and $P<0.001$, respectively). HU slightly but not significantly diminished the Δψm of the rat mesenteric arteries.

Effects of HU on mitochondrial permeability transition

To further investigate mitochondrial dysfunction and diminished Δψm, we evaluated mPTP opening in rat cerebral and mesenteric arterial VSMCs (**Fig. 4**), which allows for the diffusion of small ions across the mitochondrial inner membrane. mPTP opening increased in HU rat cerebral arteries ($P<0.01$). Both Apo and MT decreased mPTP opening induced by HU ($P<0.05$ and $P<0.01$, respectively). mPTP opening was not affected by HU in the rat mesenteric arteries.

Effects of HU on mitochondrial RCR

Mitochondrial RCR is a critical parameter of mitochondrial function and reflects the redox state of the system. HU for 4 wk decreased mitochondrial O^2 consumption of cerebral arteries during state 4 respiration (in the absence of ADP) and state 3 respiration (in the presence of ADP) (**Table 2**). Mitochondrial RCR of rat cerebral arterial VSMCs significantly reduced with 4 wk of HU ($P<0.001$), indicating uncoupling between mitochondrial respiration and oxidative phosphorylation (**Fig. 5*A***). Chronic treatment with Apo or MT restored mitochondrial RCR ($P<0.01$ and $P<0.01$, respectively). HU decreased RCR of rat mesenteric arterial VSMCs slightly but not significantly (Fig. 5*B*).

Effects of HU on mitochondrial antioxidative enzyme activities

To determine whether HU alters the antioxidative system in vascular mitochondria, enzymatic activities of MnSOD and GPx were detected in mitochondrial fractions from rat cerebral and mesenteric arterial VSMCs (**Fig. 6**). We found that both MnSOD and GPx activities in cerebral arteries significantly decreased with HU ($P<0.05$ and $P<0.001$, respectively). We also examined MnSOD and GPx activities in vascular mitochondria of rats treated with Apo or MT, and found that both antioxidants promoted significant recovery of MnSOD and GPx activity in the HU + Apo and HU + MT rat cerebral arteries ($P<0.05$ and $P<0.01$ for MnSOD, respectively; $P<0.01$ and $P<0.001$ for GPx, respectively). MnSOD and GPx activities in the mesenteric arteries were slightly but not significantly affected by either HU or Apo or MT.

Effects of HU on mitochondrial MnSOD and GPx-1 expression

To investigate the underlying mechanism of altered MnSOD and GPx activity, we examined the protein abundance of mitochondrial MnSOD and GPx-1 in rat cerebral and mesenteric VSMCs (**Fig. 7**). Compared with the control rats, the HU rats showed a significant decrease of MnSOD and GPx-1 protein levels in cerebral VSMCs ($P<0.001$ for MnSOD and GPx-1), which were partially restored by Apo and MT ($P<0.001$ and $P<0.001$ for MnSOD and GPx-1). However, the protein

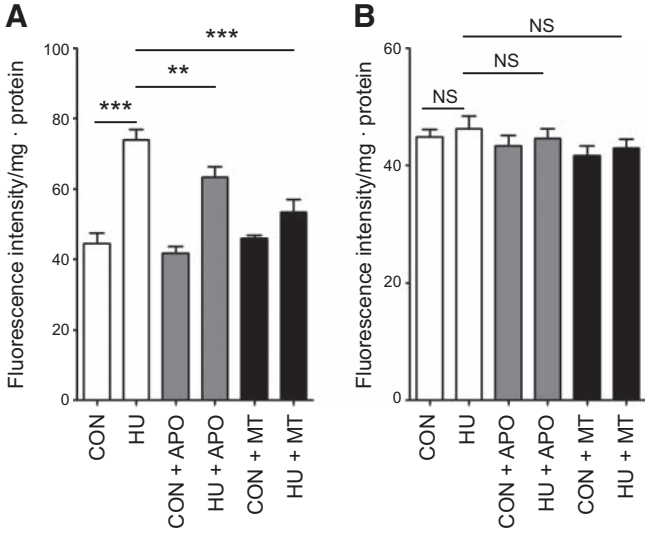

Figure 2. Effects of HU on mitochondrial ROS levels in rat cerebral (*A*) and mesenteric (*B*) VSMCs. Values are means ± SEM. $^{**}P < 0.01$, $^{***}P < 0.001$ for HU.

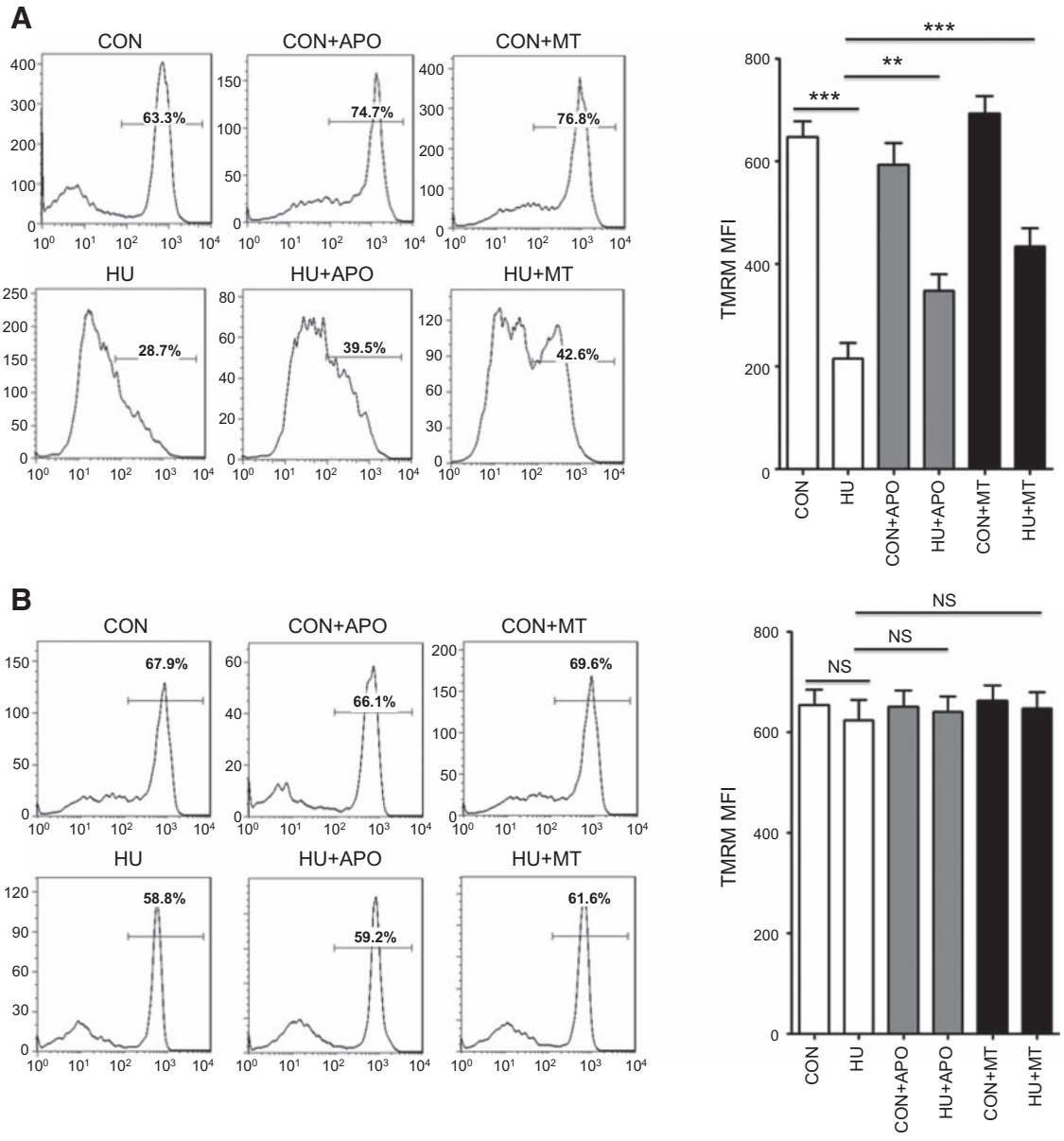

Figure 3. Effects of HU on Δψm in rat cerebral (*A*) and mesenteric (*B*) VSMCs. Results are expressed as MFI. Values are means ± SEM. $^{**}P < 0.01$, $^{***}P < 0.001$.

level of mitochondrial MnSOD and GPx-1 in HU rat mesenteric VSMCs was not altered.

Effects of HU on lipid oxidation in vascular mitochondria

Because HU damages the vascular mitochondrial oxidative defense system, we postulated that HU may provoke oxidative damage to cerebrovascular mitochondria. To test this hypothesis, we examined the levels of lipid peroxidation in vascular mitochondria isolated from Con and HU rat cerebral and mesenteric arterial VSMCs (**Fig. 8**). Concentrations of MDA, a marker for lipid peroxidation, were significantly elevated in cerebrovascular mitochondria prepared from the HU rats compared with the Con rats ($P<0.01$). Both Apo and MT therapy decreased MDA levels in HU rat cerebral arteries ($P<0.05$ and $P<0.01$, respectively). MDA levels were not affected by either HU or Apo or MT.

DISCUSSION

The results of this study suggest, for the first time to the best of the authors' knowledge, that HU results in mitochondrial dysfunction in rat cerebral arterial VSMCs. Both NADPH oxidase inhibition with Apo and mitochondria-targeted antioxidant MT restored mitochondrial function. These data indicate that mitochondrial dysfunction during microgravity may participate in cerebrovascular oxidative injury.

Cardiovascular deconditioning and consequent orthostatic intolerance complicate manned spaceflight

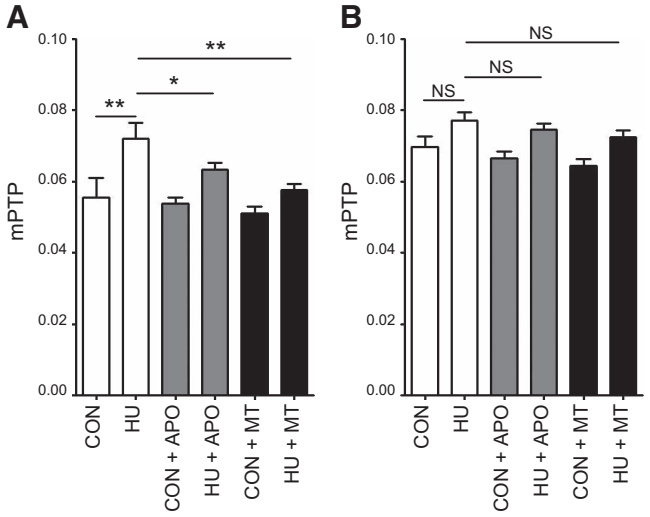

Figure 4. Effects of HU on mPTP opening in rat cerebral (*A*) and mesenteric (*B*) VSMCs. Values are means ± SEM. $*P < 0.05$, $**P < 0.01$.

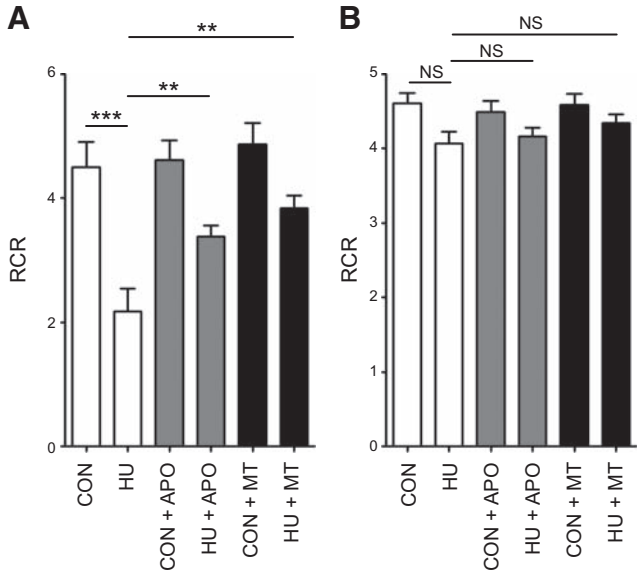

Figure 5. Effects of HU on mitochondrial RCR in rat cerebral (*A*) and mesenteric (*B*) VSMCs. Values are means ± SEM. $**P < 0.01$, $***P < 0.001$.

(1–4). Even though contrary results were reported from a study examining spaceflight mice (26), evidence from studies using HU rats indicate that contractile responses to vasoconstrictors are enhanced and endothelium-dependent relaxation is attenuated in cerebral arteries (1, 2). Despite reports from numerous studies (1, 2, 11, 16), a clear process remains to be elucidated. In our previous work, we found that L-RAS participates in HU rat cerebrovascular response regulation through modulation of the NOS-NO system (16). We also postulated that vascular oxidative stress injury is an underlying mechanism of changes in the NOS–NO system because of increased levels of $O_2^{\cdot -}$ in HU rat cerebral arteries. NADPH oxidase accounts for the enhanced vascular $O_2^{\cdot -}$ production and impaired endothelium-dependent relaxation of HU rat cerebral arteries, and NADPH oxidase inhibition with Apo reverses vascular responses to vasoconstrictors and vasodilators (11). However, the cellular mechanism of vascular oxidative stress injury during microgravity remains to be established.

NADPH oxidases have been considered the most important sources of vascular ROS and contribute to vascular functional and structural alterations in cardiovascular disorders (27, 28). However, these studies did not consider mitochondria, another major source of ROS (29, 30). The mitochondrial RCR is a critical parameter in the study of overall mitochondrial function and reflects the redox state of the system, and, therefore, the tendency of electrons to leak O^2 to form $O_2^{\cdot -}$. Mitochondrial $\Delta\psi m$ across the inner membrane represents the balance between the reduction potential of the proton pumps in the electron transport system and the rate of ion conductance back across the membrane into the matrix. The opening of mPTP leads to mitochondrial dysfunction (31). In the current study, we found decreased $\Delta\psi m$ and RCR and increased mPTP opening in HU rat VSMCs isolated from cerebral arteries, but not in mesenteric arteries. These findings indicate that mPTP opening causes the loss of $\Delta\psi m$ and increased mitochondrial ROS in HU rat cerebral arterial VSMCs. These alterations in mitochondria may result in vascular oxidative stress in HU rat cerebral arteries. The differential changes observed in mitochondrial function are consistent with previous studies that have documented

TABLE 2. *State 3 and state 4 respiration parameters of mitochondria from rat cerebral and mesenteric arterial VSMCs by study group*

	Cerebral arterial VSMCs		Mesenteric arterial VSMCs	
Group	State 3	State 4	State 3	State 4
Con	15.57 ± 0.59	3.46 ± 0.24	16.61 ± 0.57	3.63 ± 0.14
HU	6.24 ± 0.32	2.88 ± 0.18	14.06 ± 0.44	3.46 ± 0.18
Con + Apo	16.02 ± 0.61	3.48 ± 0.21	15.26 ± 0.63	3.31 ± 0.19
HU + Apo	9.79 ± 0.53	2.91 ± 0.17	14.39 ± 0.39	3.46 ± 0.22
Con + MT	16.49 ± 0.78	3.39 ± 0.23	14.76 ± 0.53	3.29 ± 0.16
HU + MT	11.83 ± 0.49	3.09 ± 0.15	14.60 ± 0.65	3.37 ± 0.18

State 3: respiration with ADP; state 4: respiration without ADP. Respiration is expressed as nanomoles of O_2 per milligram protein per minute. Values are means ± SEM (n=8/group).

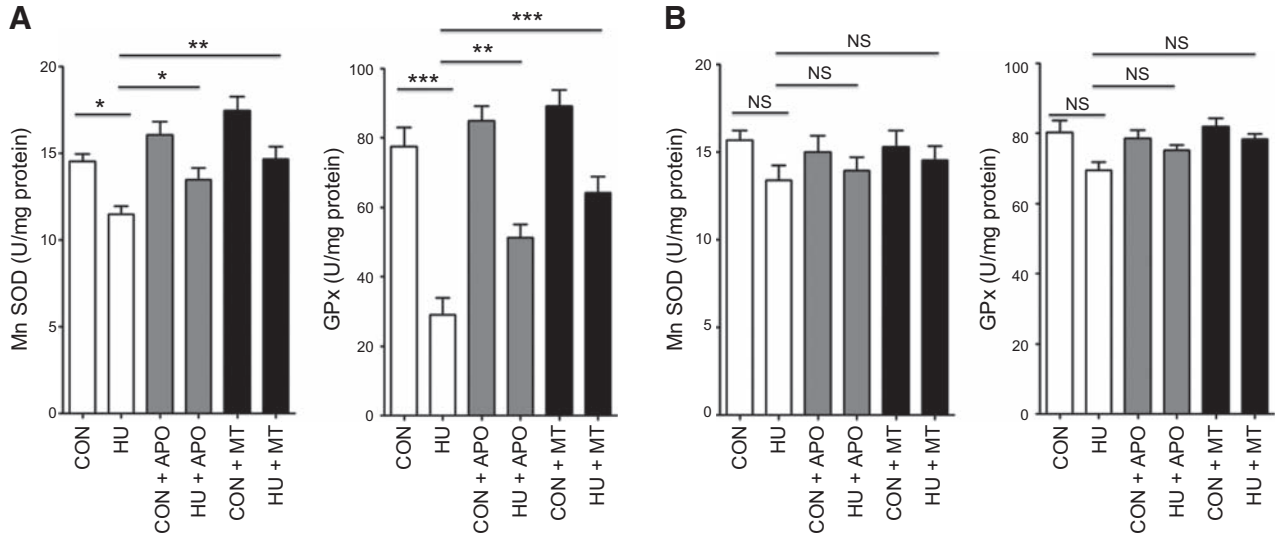

Figure 6. Effects of HU on mitochondrial MnSOD and GPx in rat cerebral (*A*) and mesenteric (*B*) VSMCs. Values are means ± SEM. $*P < 0.05$, $**P < 0.01$, $***P < 0.001$.

differential adaptations during simulated microgravity (1, 2). Mitochondrial dysfunction in HU rat cerebral arteries tended to produce more mitochondrial ROS in this study. These phenomena may be partially explained by direct oxidative damage to mitochondrial complexes, which has been shown to increase mitochondrial ROS production (32).

There is crosstalk between mitochondria and NADPH oxidases that may represent a feed-forward vicious cycle of ROS production (33). Mitochondrial dysfunction has been reported to contribute to vascular oxidative stress and vasoreactivity alterations (34–36). Although further evidence is needed, structural changes in mitochondria have been found in simulated microgravity, and mitochondrial disassembly in vascular endothelial cells (24), mitochondria swelling and vacuolation in the kidney (37), and higher mitochondrial volume densities and mitochondria-to-myofibril ratios in myocardium (38) have been observed. However, evidence of mitochondrial dysfunction remains scare, and whether dysfunctional mitochondria contribute to vascular oxidative stress injury is unknown.

In the current study, we found that vascular mitochondria were dysfunctional, and mitochondrial ROS levels increased in rat cerebral, but not mesenteric, arterial VSMCs. The results also indicate that HU-induced mitochondrial dysfunction was dependent on activation of vascular NADPH oxidases. Both Apo and MT prevented mitochondrial dysfunction and decreased mitochondrial ROS production induced by HU. These data indicate that there was interplay between NADPH oxidase and mitochondria in simulated microgravity-induced mitochondrial dysfunction. Although a depressed NOS–NO system has been reported to impair mitochondrial biogenesis and cause defunct fission/fusion and autophagy profiles within the aorta (39), the underlying mechanisms of mitochondrial dysfunction during HU remain to be established.

Mitochondria have the highest levels of antioxidants in cells and play important roles in the maintenance of cellular redox status. There are 3 different isoforms of SOD in mammals (40): cytoplasmic Cu/ZnSOD, mitochondrial MnSOD, and extracellular Cu/ZnSOD. Because of its subcellular localization, mitochondrial MnSOD is considered the first line of defense against oxidative stress. It protects NO and mitochondrial proteins from injury from $O_2^{\cdot -}$ and therefore plays crucial roles in preventing cardiovascular disorders (41–44). GPx reductively inactivates peroxides, using glutathione as a source of reducing equivalents. It is another major intracellular antioxidant enzyme that is found in the cytoplasm and mitochondria (45). In the current study, we observed decreased activity of MnSOD and GPx in 4-wk-old HU rat cerebral, but not mesenteric, arterial VSMCs. The altered MnSOD and GPx activity may be attributable to decreased protein expression of mitochondrial MnSOD and GPx-1 in HU rat cerebral arteries in this work. The activity and expression of both antioxidative enzymes were also restored by Apo and MT. Taken together, these data suggest an attenuated mitochondrial antioxidant system in rat cerebral arteries during HU.

Mitochondrial dysfunction and oxidative stress have been implicated in the pathogenesis of aging and cardiovascular disorders. During aging, dysfunctional mitochondria provoke oxidative stress, which disturbs the cellular redox balance (46). MnSOD and GPx-1 deficiency increased mitochondrial oxidative stress and aggravated age-dependent vascular dysfunction, which was more pronounced in aged *MnSOD*$^{+/-}$ and *GPx-1*$^{-/-}$ mice (47, 48). The roles of mitochondrial dysfunction in the regulation of vascular NADPH oxidases and the development of hypertension have been well documented (49). MT and MnSOD overexpression decrease mitochondrial and cellular $O_2^{\cdot -}$ reduces cellular NADPH oxidase activ-

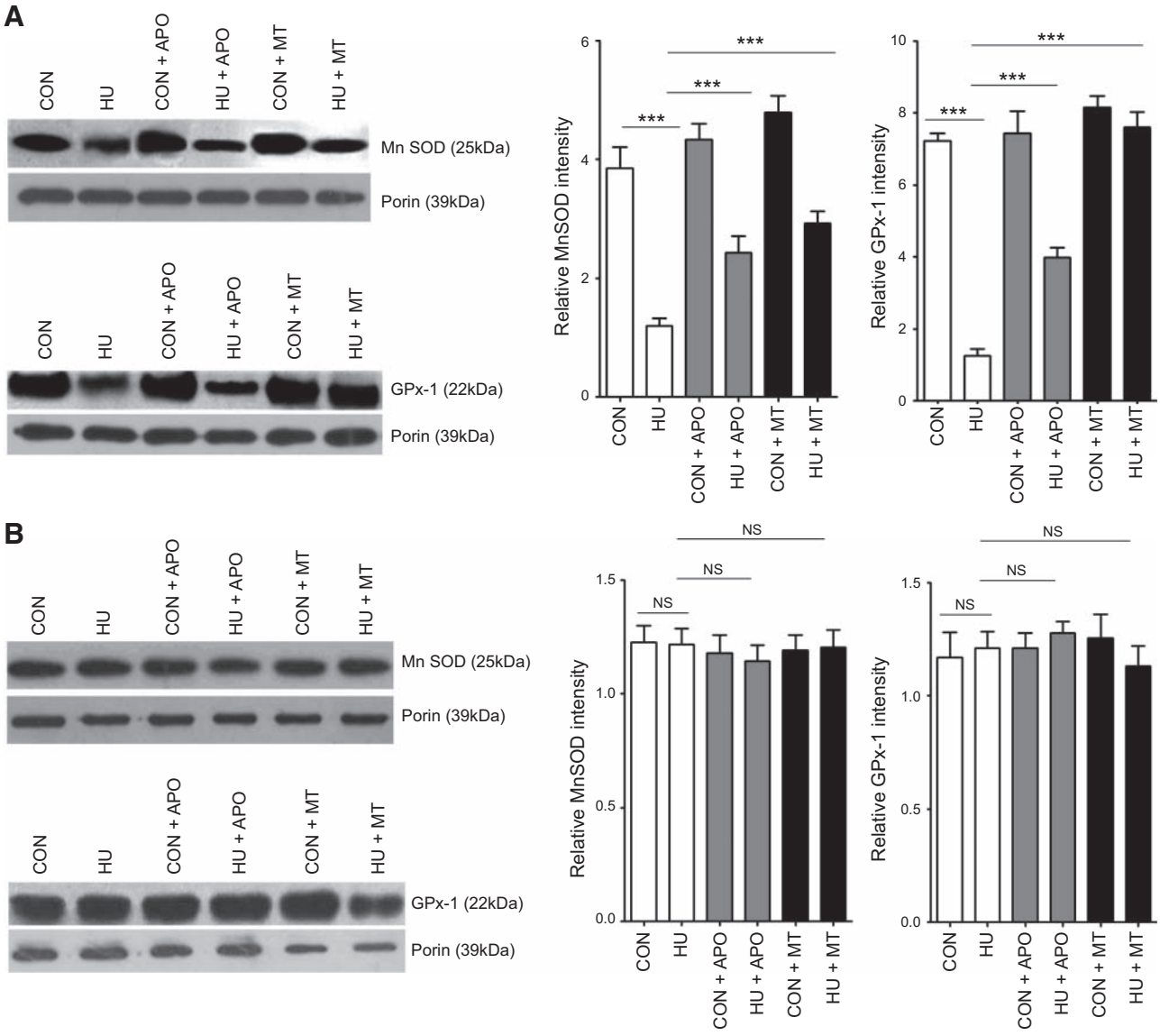

Figure 7. Effects of HU on protein abundance of mitochondrial MnSOD and GPx-1 in rat cerebral (*A*) and mesenteric (*B*) arteries. Left panels: Western blot analysis. Right panels: relative expression of proteins after normalization to porin expression. Values are means ± SEM. ***$P < 0.001$.

ity and improves endothelium-dependent relaxation in Ang II-induced and DOCA salt hypertension (43). The molecular mechanisms of Ang II actions involve NADPH oxidases stimulation and mitochondrial dysfunction, which accounts for the development of endothelial dysfunction and hypertension (18). Mitochondrial dysfunction is also involved in the development of heart failure and atherosclerosis (50, 51), and scavenging mitochondrial ROS protect a pressure-overloaded heart from failure (52). Therefore, mitochondrial dysfunction in cerebral arteries during simulated microgravity is a very important phenomenon because it may have a functional role in cerebrovascular functional remodeling induced by microgravity, a possibility that merits further investigation.

As for the mesenteric arteries, we did not found mitochondrial dysfunction in HU rats. Although the different changes in VSMCs ion channels (7–9) secondary to gravitational pressure gradient shifts in the circulation (4) have been indicated in differential vascular structural and functional remodeling during microgravity, the underlying mechanism remains to be established. Further studies are needed to investigate this question.

The findings of the current study suggest that simulated microgravity results in mitochondrial dysfunction and oxidative injury of HU rat cerebral but not mesenteric arterial VSMCs. There appears to be crosstalk between cytoplasmic NADPH oxidases and mitochondria in mitochondrial dysfunction. Further studies are needed to elucidate the time course characteristics of mitochondrial dysfunction during HU and provide information on the functional roles of mitochondrial dysfunction in vascular structural and functional remodeling during microgravity.

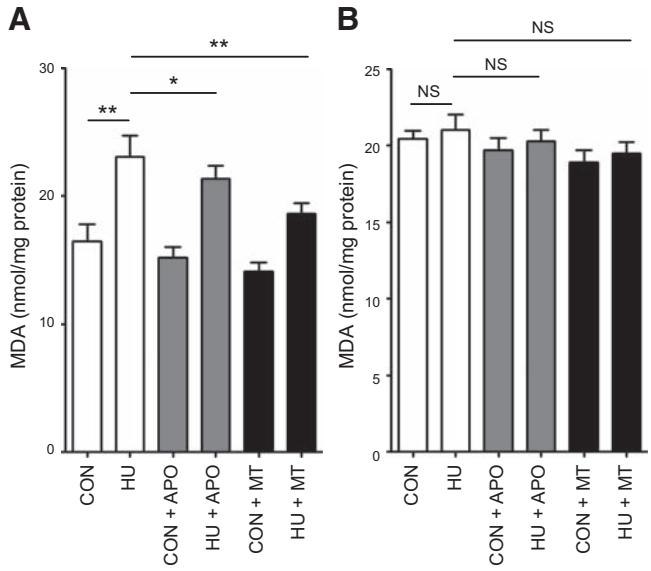

Figure 8. Effects of HU on mitochondrial lipid peroxidation of MDA in rat cerebral (*A*) and mesenteric (*B*) VSMCs. Values are means ± SEM. $*P < 0.05$, $**P < 0.01$.

This work was supported by the National Natural Science Foundation of China (81101468 and 81030002/H02) and the Beijing NOVO Program (XX2013105). The authors declare no conflicts of interest.

REFERENCES

1. Zhang, L. F. (2013) Region-specific vascular remodeling and its prevention by artificial gravity in weightless environment. *Eur. J. Appl. Physiol.* **113,** 2873–2895
2. Zhang, L. F. (2001) Vascular adaptation to microgravity: what have we learned? *J. Appl. Physiol.* **91,** 2415–2430
3. Convertino, V. A. (2002) Mechanisms of microgravity induced orthostatic intolerance: implications for effective countermeasures. *J. Gravit. Physiol.* **9,** 1–13
4. Hargens, A. R., and Watenpaugh, D. E. (1996) Cardiovascular adaptation to spaceflight. *Med. Sci. Sports Exerc.* **28,** 977–982
5. Cheng, J. H., Boscolo, M., Lin, L. J., Bai, Y. G., Zhang, X., Ma, J., and Zhang, L. F. (2009) [Comparison of biomechanical behavior of cerebral and mesenteric small arteries of simulated microgravity rats.] *Sheng Li Xue Bao* **61,** 386–394
6. Lin, L. J., Gao, F., Bai, Y. G., Bao, J. X., Huang, X. F., Ma, J., and Zhang, L. F. (2009) Contrasting effects of simulated microgravity with and without daily −Gx gravitation on structure and function of cerebral and mesenteric small arteries in rats. *J. Appl. Physiol.* **107,** 1710–1721
7. Xue, J. H., Chen, L. H., Zhao, H. Z., Pu, Y. D., Feng, H. Z., Ma, Y. G., Ma, J., Chang, Y. M., Zhang, Z. M., and Xie, M. J. (2011) Differential regulation and recovery of intracellular Ca2+ in cerebral and small mesenteric arterial smooth muscle cells of simulated microgravity rat. *PLoS One* **6,** e19775
8. Xue, J. H., Zhang, L. F., Ma, J., and Xie, M. J. (2007) Differential regulation of L-type Ca2+ channels in cerebral and mesenteric arteries after simulated microgravity in rats and its intervention by standing. *Am. J. Physiol. Heart Circ. Physiol.* **293,** H691–H701
9. Fu, Z. J., Xie, M. J., Zhang, L. F., Cheng, H. W., and Ma, J. (2004) Differential activation of potassium channels in cerebral and hindquarter arteries of rats during simulated microgravity. *Am. J. Physiol. Heart Circ. Physiol.* **287,** H1505–H1515
10. Ren, X. L., Zhang, R., Zhang, Y. Y., Liu, H., Yu, J. W., Cai, Y., Wang, Z. C., Purdy, R. E., and Ma, J. (2011) Nitric oxide synthase activity in the abdominal aorta of rats is decreased after 4 weeks of simulated microgravity. *Clin. Exp. Pharmacol. Physiol.* **38,** 683–687
11. Zhang, R., Ran, H. H., Ma, J., Bai, Y. G., and Lin, L. J. (2012) NAD(P)H oxidase inhibiting with apocynin improved vascular reactivity in tail-suspended hindlimb unweighting rat. *J. Physiol. Biochem.* **68,** 99–105
12. Zhang, R., Jia, G., Bao, J., Zhang, Y., Bai, Y., Lin, L., Tang, H., and Ma, J. (2008) Increased vascular cell adhesion molecule-1 was associated with impaired endothelium-dependent relaxation of cerebral and carotid arteries in simulated microgravity rats. *J. Physiol. Sci.* **58,** 67–73
13. Kang, H., Fan, Y., Sun, A., Jia, X., and Deng, X. (2013) Simulated microgravity exposure modulates the phenotype of cultured vascular smooth muscle cells. *Cell Biochem. Biophys.* **66,** 121–130
14. Bao, J. X., Zhang, L. F., and Ma, J. (2007) Angiotensinogen and AT1R expression in cerebral and femoral arteries during hindlimb unloading in rats. *Aviat. Space Environ. Med.* **78,** 852–828
15. Gao, F., Zhang, L. F., Huang, W. Q., and Sun, L. (2007) [Chronic blockade of angiotensin II type 1 receptor cannot completely prevent structural adaptation in vessels of simulated weightless rats.] *Sheng Li Xue Bao* **59,** 821–830
16. Zhang, R., Bai, Y. G., Lin, L. J., Bao, J. X., Zhang, Y. Y., Tang, H., Cheng, J. H., Jia, G. L., Ren, X. L., and Ma, J. (2009) Blockade of AT1 receptor partially restores vasoreactivity, NOS expression, and superoxide levels in cerebral and carotid arteries of hindlimb unweighting rats. *J. Appl. Physiol.* **106,** 251–258
17. Zhang, R., Ran, H. H., Gao, Y. L., Ma, J., Huang, Y., Bai, Y. G., and Lin, L. J. (2010) Differential vascular cell adhesion molecule-1 expression and superoxide production in simulated microgravity rat vasculature. *EXCLI J.* **9,** 195–204
18. Doughan, A. K., Harrison, D. G., and Dikalov, S. I. (2008) Molecular mechanisms of angiotensin II-mediated mitochondrial dysfunction: linking mitochondrial oxidative damage and vascular endothelial dysfunction. *Circ. Res.* **102,** 488–496
19. Dikalov, S. I., Nazarewicz, R. R., Bikineyeva, A., Hilenski, L., Lassègue, B., Griendling, K. K., Harrison, D. G., and Dikalova, A. E. (2014) Nox2-induced production of mitochondrial superoxide in angiotensin II: mediated endothelial oxidative stress and hypertension. *Antioxid. Redox Signal.* **20,** 281–294
20. Gao, L., Laude, K., and Cai, H. (2008) Mitochondrial pathophysiology, reactive oxygen species, and cardiovascular diseases. *Vet. Clin. North Am. Small Anim. Pract.* **38,** 137–155
21. Zang, Q., Maass, D. L., White, J., and Horton, J. W. (2007) Cardiac mitochondrial damage and loss of ROS defense after burn injury: the beneficial effects of antioxidant therapy. *J. Appl. Physiol.* **102,** 103–112
22. Chrissobolis, S., Didion, S. P., Kinzenbaw, D. A., Schrader, L. I., Dayal, S., Lentz, S. R., and Faraci, F. M. (2008) Glutathione peroxidase-1 plays a major role in protecting against angiotensin II-induced vascular dysfunction. *Hypertension* **51,** 872–877
23. Zhan, C. D., Sindhu, R. K., Pang, J., Ehdaie, A., and Vaziri, N. D. (2004) Superoxide dismutase, catalase and glutathione peroxidase in the spontaneously hypertensive rat kidney: effect of antioxidant-rich diet. *J. Hypertens.* **22,** 2025–2033
24. Morbidelli, L., Monici, M., Marziliano, N., Cogoli, A., Fusi, F., Waltenberger, J., and Ziche, M. (2005) Simulated hypogravity impairs the angiogenic response of endothelium by up-regulating apoptotic signals. *Biochem. Biophys. Res. Commun.* **334,** 491–499
25. Dikalov, S. I., and Nazarewicz, R. R. (2013) Angiotensin II-induced production of mitochondrial reactive oxygen species: potential mechanisms and relevance for cardiovascular disease. *Antioxid. Redox Signal.* **19,** 1085–1094
26. Taylor C. R., Hanna M., Behnke B. J., Stabley J. N., McCullough D. J., and Davis, R. T. 3rd, Ghosh P., Papadopoulos A., Muller-Delp J. M., and Delp M. D. (2013) Spaceflight-induced alterations in cerebral artery vasoconstrictor, mechanical, and structural properties: implications for elevated cerebral perfusion and intracranial pressure. *FASEB J.* **27,** 2282–2292
27. Lassègue, B., San Martín, A., and Griendling, K. K. (2012) Biochemistry, physiology, and pathophysiology of NADPH oxidases in the cardiovascular system. *Circ. Res.* **110,** 1364–1390
28. Brandes, R. P. (2010) Vascular functions of NADPH oxidases. *Hypertension* **56,** 17–21
29. Han, D., Antunes, F., Canali, R., Rettori, D., and Cadenas, E. (2003) Voltage-dependent anion channels control the release of

superoxide anion from mitochondria to cytosol. *J. Biol. Chem.* **278,** 5557–5563
30. Turrens, J. F. (2003) Mitochondrial formation of reactive oxygen species. *J. Physiol.* **552,** 335–344
31. Javadov, S., Karmazyn, M., and Escobales, N. (2009) Mitochondrial permeability transition pore opening as a promising therapeutic target in cardiac diseases. *J. Pharmacol. Exp. Ther.* **330,** 670–678
32. Panov, A., Dikalov, S., Shalbuyeva, N., Taylor, G., Sherer, T., and Greenamyre, J. T. (2005) Rotenone model of Parkinson disease: multiple brain mitochondria dysfunctions after short term systemic rotenone intoxication. *J. Biol. Chem.* **280,** 42026–42035
33. Dikalov, S. (2011) Cross talk between mitochondria and NADPH oxidases. *Free Radic. Biol. Med.* **51,** 1289–1301
34. Freed, J. K., and Gutterman, D. D. (2013) Mitochondrial reactive oxygen species and vascular function: less is more. *Arterioscler. Thromb. Vasc. Biol.* **33,** 673–675
35. Xi, Q., Cheranov, S. Y., and Jaggar, J. H. (2005) Mitochondria-derived reactive oxygen species dilate cerebral arteries by activating Ca2+ sparks. *Circ. Res.* **97,** 354–362
36. Kluge, M. A., Fetterman, J. L., and Vita, J. A. (2013) Mitochondria and endothelial function. *Circ. Res.* **112,** 1171–1188
37. Ding, Y., Zou, J., Li, Z., Tian, J., Abdelalim, S., Du, F., She, R., Wang, D., Tan, C., Wang, H., Chen, W., Lv, D., and Chang, L. (2011) Study of histopathological and molecular changes of rat kidney under simulated weightlessness and resistance training protective effect. *PLoS One* **6,** e20008
38. Goldstein M. A., Edwards R. J., and Schroeter, J. P. (1992) Cardiac morphology after conditions of microgravity during COSMOS 2044. *J. Appl. Physiol.* (1985) **73,** 94S–100S.
39. Miller, M. W., Knaub, L. A., Olivera-Fragoso, L. F., Keller, A. C., Balasubramaniam, V., Watson, P. A., and Reusch, J. E. (2013) Nitric oxide regulates vascular adaptive mitochondrial dynamics. *Am. J. Physiol. Heart Circ. Physiol.* **304,** H1624–H1633
40. Fukai, T., and Ushio-Fukai, M. (2011) Superoxide dismutases: role in redox signaling, vascular function, and diseases. *Antioxid. Redox Signal.* **15,** 1583–1606
41. Faraci, F. M., and Didion, S. P. (2004) Vascular protection: superoxide dismutase isoforms in the vessel wall. *Arterioscler. Thromb. Vasc. Biol.* **24,** 1367–1373
42. Miller, J. D., Peotta, V. A., Chu, Y., Weiss, R. M., Zimmerman, K., Brooks, R. M., and Heistad, D. D. (2010) MnSOD protects against COX1-mediated endothelial dysfunction in chronic heart failure. *Am. J. Physiol. Heart Circ. Physiol.* **298,** H1600–H1607
43. Dikalova, A. E., Bikineyeva, A. T., Budzyn, K., Nazarewicz, R. R., McCann, L., Lewis, W., Harrison, D. G., and Dikalov, S. I. (2010) Therapeutic targeting of mitochondrial superoxide in hypertension. *Circ. Res.* **107,** 106–116
44. Afolayan, A. J., Eis, A., Teng, R. J., Bakhutashvili, I., Kaul, S., Davis, J. M., and Konduri, G. G. (2012) Decreases in manganese superoxide dismutase expression and activity contribute to oxidative stress in persistent pulmonary hypertension of the newborn. *Am. J. Physiol. Lung Cell. Mol. Physiol.* **303,** L870–L879
45. Handy, D. E., Lubos, E., Yang, Y., Galbraith, J. D., Kelly, N., Zhang, Y. Y., Leopold, J. A., and Loscalzo, J. (2009) Glutathione peroxidase-1 regulates mitochondrial function to modulate redox-dependent cellular responses. *J. Biol. Chem.* **284,** 11913–11921
46. Dai, D. F., Rabinovitch, P. S., and Ungvari, Z. (2012) Mitochondria and cardiovascular aging. *Circ. Res.* **110,** 1109–1124
47. Wenzel, P., Schuhmacher, S., Kienhöfer, J., Müller, J., Hortmann, M., Oelze, M., Schulz, E., Treiber, N., Kawamoto, T., Scharffetter-Kochanek, K., Münzel, T., Bürkle, A., Bachschmid, M. M., and Daiber, A. (2008) Manganese superoxide dismutase and aldehyde dehydrogenase deficiency increase mitochondrial oxidative stress and aggravate age-dependent vascular dysfunction. *Cardiovasc. Res.* **80,** 280–289
48. Oelze, M., Kröller-Schön, S., Steven, S., Lubos, E., Doppler, C., Hausding, M., Tobias, S., Brochhausen, C., Li, H., Torzewski, M., Wenzel, P., Bachschmid, M., Lackner, K. J., Schulz, E., Münzel, T., and Daiber, A. (2014) Glutathione peroxidase-1 deficiency potentiates dysregulatory modifications of endothelial nitric oxide synthase and vascular dysfunction in aging. *Hypertension* **63,** 390–396
49. Dikalov, S. I., and Ungvari, Z. (2013) Role of mitochondrial oxidative stress in hypertension. *Am. J. Physiol. Heart Circ. Physiol.* **305,** H1417–H1427
50. Tsutsui, H., Kinugawa, S., and Matsushima, S. (2009) Mitochondrial oxidative stress and dysfunction in myocardial remodelling. *Cardiovasc. Res.* **81,** 449–456
51. Madamanchi, N. R., and Runge, M. S. (2007) Mitochondrial dysfunction in atherosclerosis. *Circ. Res.* **100,** 460–473
52. Dai D. F., Hsieh E. J., Liu Y., Chen T., Beyer R. P., Chin M. T., MacCoss M. J., Rabinovitch P. S. (2012) Mitochondrial proteome remodelling in pressure overload-induced heart failure: the role of mitochondrial oxidative stress. *Cardiovasc. Res.* **93**: 79–88

Received for publication November 25, 2013.
Accepted for publication February 24, 2014.